패턴이 있는 TFT-LCD 패널의 결함검사를 위하여 근접패턴비교와 경계확장 알고리즘을 이용한 자동광학검사기(AOI) 개발

Development of AOI(Automatic Optical Inspection) System for Defect Inspection of Patterned TFT-LCD Panels Using Adjacent Pattern Comparison and Border Expansion Algorithms

강 성 범*, 이 명 선, 박 희 재
(Sung-Bum Kang, Myung-Sun Lee, and Heui-Jae Pahk)

Abstract : This paper presents an overall image processing approach of defect inspection of patterned TFT-LCD panels for the real manufacturing process. A prototype of AOI(Automatic Optical Inspection) system which is composed of air floating stage and multi line scan cameras is developed. Adjacent pattern comparison algorithm is enhanced and used for pattern elimination to extract defects in the patterned image of TFT-LCD panels. New region merging algorithm which is based on border expansion is proposed to identify defects from the pattern eliminated defect image. Experimental results show that a developed AOI system has acceptable performance and the proposed algorithm reduces environmental effects and processing time effectively for applying to the real manufacturing process.

Keywords : AOI(Automatic Optical Inspection), defect inspection, border expansion

I. Introduction

Over the past few years, the tide of display market has turned from Cathode Ray Tube(CRT) to Flat Panel Display(FPD). Among FPDs, Thin film transistor-liquid crystal display(TFT-LCD) deserves our attention due to their full-color display capability, low power consumption and light weight. Moreover, it has become increasingly popular with price reduction and quality improvement during the last two years.

With the growth of LCD market, it is certainly needed to enlarge production facilities with ensuring the display quality. With the price reduction of LCD, the prime cost reduction has been raised as the most important issue. Especially, a competitive prime cost between flat panel display companies has become more serious for the coming mass market of digital TV. Defect inspection is a critical part for prime cost reduction in manufacturing process. Especially a machine vision approach is widely used for precise, repeatable, high-speed inspection evaluation.

This paper presents a research on developing an AOI(Automatic Optical Inspection) system to detect micro defects of TFT-LCD panels which is applicable to the real manufacturing process after 7th-generation glass. The key performances of AOI system such as minimum detectable defect size and tact time are not fixed but vary according to production line and companies. However, the general minimum defect size is 8μm which must be detected for LCD color filter and the general tact time for glass scanning with real-time processing is 20 to 30 seconds for 5th-generation(1250mm×1100mm) glass.

The ultimate purpose of this research is to develop AOI system to inspect the defects in the minimum size of 8μm within 30 seconds excluding glass loading and unloading for 5th-generation glass. The main effort of the research is placed on the development of overall image processing algorithm for defect inspection which is accurate and fast enough to apply in the real manufacturing process.

* 책임저자(Corresponding Author)
논문접수 : 2008. 1. 31., 채택확정 : 2008. 2. 24.
강성범 : ㈜에스엔유프리시젼(sbkang@snuprecision.com)
이명선, 박희재 : 서울대학교 기계항공공학부
(hansol2@snu.ac.kr/hjpark@snu.ac.kr)
※ 본 연구는 ㈜에스엔유프리시젼의 지원으로 수행되었음.

II. Image Processing for Defect Inspection

There are four image processing steps for defect detection and classification of patterned TFT-LCD panels. First, pattern elimination step: Image processing for pattern elimination to get only defect images from the patterned image is required because LCD panels have a pattern. Second, defect labeling step: All the connected pixels in the defect image have to be labeled with a unique number. Third, defect feature extraction step: Quantitative of defect feature information such as defect size, area and position have to be extracted. We call the second and third steps as 'Defect Identification'. Last, defect classification step: Identified defects are classified and this information is used for process quality control.

Step 1: Pattern Elimination

There are various defect detection methods of patterned TFT-LCD panels. Adjacent pattern comparison method was developed by Yoda[20]. An automatic vision system based on pattern matching algorithm has developed by Sokolov[16]. An image subtraction and Fourier filtering for detecting defect are developed by Nakashima[12]. Parallel grayscale image comparison method is developed by Onishi[14]. A singular value decomposition method for defect detection of TFT-LCD is developed by Lu[10]. A global one-dimensional Fourier-based image reconstruction scheme is proposed by Tsai[19].

Line scan type is used for large size of LCD panels and it needs precise environment control such as illumination and vibration. Fast processing is necessary to reduce tact time in real manufacturing application. Adjacent pattern comparison

algorithm is most widely used for large size LCD panel inspection because it is insensitive to the non-uniform illumination and it doesn't need pre-stored reference image.

However, adjacent pattern comparison algorithm has several disadvantages. First, pseudo-defect can be detected because the reference is not assured to be faultless as depicted in Fig. 1(d) and (f). To solve this problem, 4-directional adjacent pattern comparison algorithm is used for detecting defect in the patterned image. Fig. 1 shows pseudo-defect elimination principle of two-directional adjacent pattern comparison algorithm.

Second, it generates noise when pattern period is not an integer value. For example, if the real pattern period of LCD glass pattern is 221um, it is 27.625px in the image for 1x optics when the CCD size 8um. It is impossible to shift 27.625px in image for pattern comparison. To solve this problem, the adjacent pattern comparison algorithm is enhanced with sub-pixel algorithm using linear interpolation between image pixel values as the following equation and Fig. 2 shows the noise reduction effect of the enhanced algorithm.

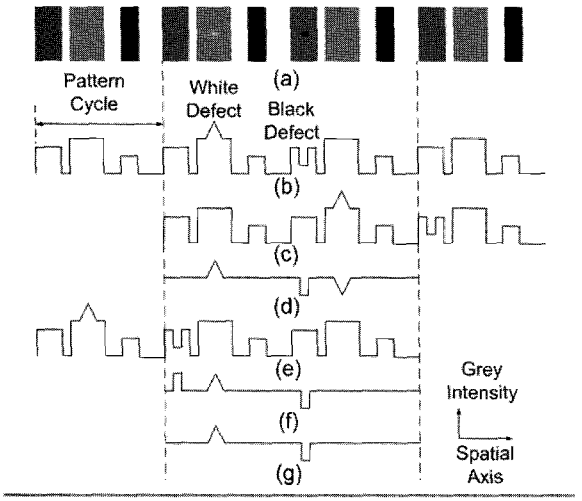

그림 1. 패턴 영상에서 결함 검출을 위한 2방향 근접 패턴 비교 알고리즘. (a) 두 개의 결함이 존재하는 결함 패턴 이미지. (b) 결함 패턴 이미지(a)에서 결함이 존재하는 수평라인에 대한 밝기 프로파일. (c) (b)를 오른쪽으로 한 사이클 이동시킨 밝기 프로파일. (d) (b)에서 (c)를 뺀 밝기 프로파일. (e) (b)를 왼쪽으로 한 사이클 이동시킨 밝기 프로파일. (f) (b)에서 (e)를 뺀 밝기 프로파일. (g) (d)와 (f)를 AND연산한 밝기 프로파일; 여기서 양수는 백결함, 음수는 흑결함을 나타낸다.

Fig. 1. 2-directional adjacent pattern comparison algorithm to detect defect in the patterned image. (a) An artificial defective image which has two defects. (b) Defective line intensity profile of (a). (c) One cycle shifted intensity profile of (b) toward the right. (d) Subtracted intensity profile of (c) form (b). (e) One cycle shifted intensity profile of (b) toward the left. (f) Subtracted intensity profile of (e) from (b). (g) AND-operated intensity profile of (d) and (f). An positive value and a negative value represent white defect and black defect, respectively.

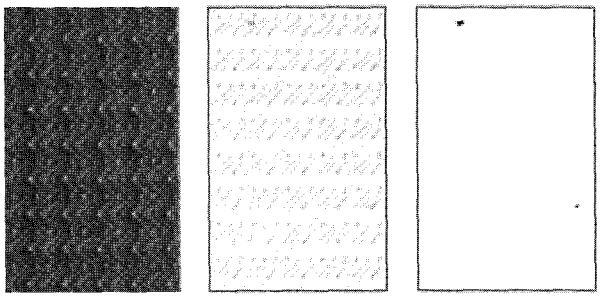

(a) (b) (c)

그림 2. 선형 보간을 이용한 서브 픽셀 처리를 통한 강화된 근접 패턴 비교 알고리즘 (a) 영상에서 한 픽셀이 8um의 해상도를 가지는 광학계를 이용하여 획득한 패턴 주기가 221um(=27.625px)인 LCD 패턴영상. (b) 2방향 근접패턴비교 알고리즘을 이용하여 패턴을 제거한 영상. (c) 서브 픽셀 수준의 강화된 패턴비교 알고리즘을 이용하여 패턴을 제거한 영상.

Fig. 2. Enhanced adjacent pattern comparison algorithm using linear interpolation based sub-pixel calculation. (a) Original LCD pattern image whose pattern period is 221um (=27.625px) (b) Pattern eliminated image using simple 2-diretional pattern comparison algorithm (c) Pattern eliminated and contrast enhanced image using enhanced adjacent pattern comparison algorithm.

$$R(x,y) = \{|I(x,y) - I(x, y,p,0)| + |I(x,y) - I(x, y, -p,0)| + |I(x,y) - I(x, y,0,p)| + |I(x,y) - I(x, y,0, -p)|\}/4 \quad (1)$$

$$I(x,y,sx,sy) = \{I(x,y,sx_i,0) \times sx_f + I(x,y,sx_i 1,0) \times (1-sx_f) + I(x,y,0,sy_i) \times sy_f + I(x,y,0,sy_i + 1) \times (1-sy_f)\}/2 \quad (2)$$

where, I(x,y) is pixel intensity value of source image at (x,y), R(x,y) is pixel intensity value of pattern eliminated image at (x,y), p is pattern period in image coordinates, I(x,y,sx,sy) is intensity value of (sx,sy) pixel shifted position from (x,y), subscript i and f represent a number above and under the decimal point.

Step 2: Defect Labeling

Each connected pixels in the defect image have to be labeled with the unique number. However, there is one problem of region division as shown in the Fig. 3. In this case, merging of adjacent regions in the defect image is required before the extraction of defect feature information because a defect can be divided into several regions and simple labeling algorithm identifies them as different defects.

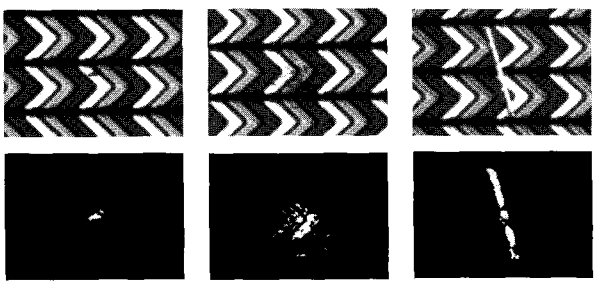

그림 3. 하나의 결함이 여러 개의 영역으로 나누어진 예.

Fig. 3. Region division examples of three defects.

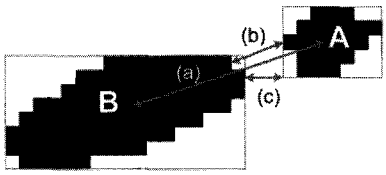

그림 4. 두 개의 영역 사이의 거리에 대한 다양한 정의. (a) 각 영역의 중심간의 거리. (b) 각 영역 경계간의 최소거리. (c) 각 영역을 감싸는 사각형간의 최소거리.

Fig. 4. Variable definitions of distance between two regions. (a) An interval of two center positions (b) A minimum interval of two borders (c) An interval of two rectangular borders.

Four-connectivity directional notation[4] is used for the border based region segmentation. Sequential local operations which label the connected components of the image is described by Rosenfeld[15]. A complex morphological operations of opening, closing and shape decomposition constituted by simple dilation and erosion is formalized by Minkowski[8]. Several graph searching algorithms[17] is used for detection of divided border.

The criterion for merging two defects is closeness. The distance between two defects can be defined in variable ways as depicted in Fig. 4. Among them, minimum distance between two borders is suitable to define the closeness of two defects and it is used for merging of adjacent defects.

Dilation and erosion algorithm is widely used to connect objects that are close to each other. However, it needs time for processing as much as defect labeling and the processing time increases linearly as merging gap. New optimal algorithm is needed for the adjacent object merging. Border based region segmentation and inner border tracing algorithm is used for defect labeling. Outer border extension algorithm is proposed for adjacent object merging. Detailed description is presented in Chapter 3.

Step 3: Defect Feature Extraction

A blob(binary large object) is an area of connected pixels with the same logical state. All pixels in an image that belong to a blob are in a foreground state. All other pixels are in a background state. In a binary image, pixels in the background have values equal to zero while every nonzero pixel is part of a binary object. Blob analysis means to detect blobs in an image and make selected measurements of those blobs. It consists of a series of processing operations and analysis functions that produce information about any 2D shape in an image.

Border tracing is used for the defect labeling. Blob analysis is performed during the border tracing step to identify defects. Defect features listed in Table 1 is extracted during blob analysis. Theses variables are used for the further processes such as review, repair and process quality control. For example, the results are used to direct glasses to repair station, with the added benefit of providing the exact coordinates of detected defect to the repair operator.

Step 4: Defect Classification

Quality control of TFT-LCD panel production is an important factor to improve product reliability. To meet the needs of quality control in every TFT-LCD manufacturing step, an inspection system is needed for defect classification. In the TFT-LCD production line, the inspection systems are installed in each process such as black matrix process, RGB process and etc. A defect detection process can be confirmed by checking AOI system in the real production line. Moreover, the information of defect classes are useful to know defect formed process exactly. Defect image learning and classification algorithm are necessary to decide a class of defect. General micro-defect classes are presented in Table 2.

표 1. 결함의 특징 정보 리스트.

Table 1. Defect feature lists.

size	width, height, area
position	defect center position in a pattern
geometric border	border length, curvature
scalar region descriptor	eccentricity, elongation, rectangularity

표 2. 마이크로 결함의 일반적 분류.

Table 2. General micro-defect classes.

ITO/BM/RGB pattern defect/overlay
ITO/BM/RGB layer pinhole
General particle or dust
Particle before/after ITO coating process
Slender(a piece of thread shaped) defect
ITO/BM layer remaining defect
A protrusion type defect
Scattered/Oily shaped defect
Over etching over ITO

Several data analysis methodologies can be used for defect image learning and classification. Data mining algorithms such as Principal Components Analysis(Hotelling, 1933) and the Linear Discriminant Analysis(Fisher, 1936) for reducing defect feature dimension are useful to reduce processing time in the case of multi-feature analysis. Back Propagation(Rumelhart, 1986) of Artificial Neural Network and Support Vector Machine(Vapnik, 1995) are widely used for data leaning and classification.

III. New Defect Blob Merging Algorithm : Border Expansion

Chains codes[4] are often used for the description of object borders. The border is defined by the coordinates of its reference pixel and the sequence of symbols corresponding to the line of the unit length in several pre-defined orientation such as chain code. Four directional chain codes are shown in Fig. 5.

1. Run-length coding of border chain code

Run length coding is quite often used to represent strings of symbols in an image matrix(for instance, FAX machines use run length coding). Run-length coding of border chain codes reduces processing time. In this research, border based segmentation and inner border tracing algorithm are used for defect labeling. During the inner border tracing, chain codes of inner border are stored in run length coding; chain code are sequentially compared and grouped together into runs of identical chain codes. An example of run length coding of inner border chain codes is shown in Fig. 6. In this example, starting pixel position of chain code tracing is X=11 and Y=4. Run length coding of inner border chain codes

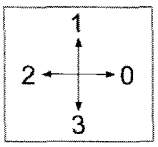

그림 5. 4-방향 연결성에 대한 방향 지시자.

Fig. 5. Directional notation of 4-connectivity.

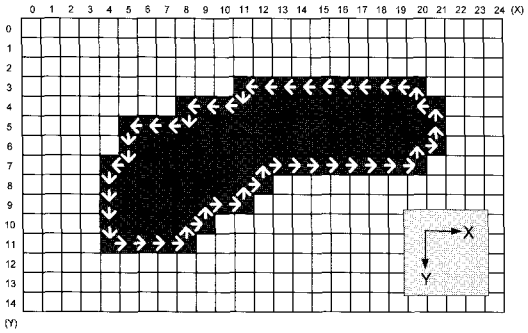

그림 6. 영역의 내부경계 체인코드의 run-length 코딩의 예.

Fig. 6. An example of run-length coding of inner border chain codes.

based on the four-connectivity is (3:1, 2:3, 3:1, 2:3, 3:2, 2:1, 3:4, 0:4, 1:1, 0:1, 1:1, 0:2, 1:1, 0:1, 1:1, 0:8, 1:1, 0:1, 1:2, 2:1, 1:1, 2:9). In this chapter, the notation of (D_N:nD_N) is used where D_N and nD_N represent chain code value and the number of D_N, respectively.

2. Chain Code Modification

Inner border chain code can be expanded by four criterions introduced in this chapter. Expanded border can be extracted from this expended chain code and it is used to find adjacent blobs.

Criterion 1: If connected two chain codes(D_N:nD_N, D_{N+1}:nD_{N+1}) are components of convex shape(Fig.7), add each number of chain codes, nD_N and nD_{N+1}, by one. A general description of two connected chain codes which represent a convex shape is (D, (D+1)%4).

Criterion 2: If connected two chain codes(D_N:nD_N, D_{N+1}:nD_{N+1}) are components of concave shape(Fig.8), reduce each number of chain codes, nD_N and nD_{N+1}, by one. A general description of two connected chain codes which represent a convex shape is (D, (D+3)%4).

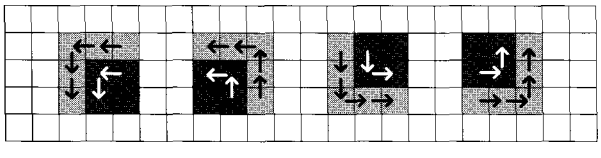

(a) (b) (c) (d)

그림 7. 반 시계 방향의 경계 추적에 있어서 체인코드 추가의 네 가지 경우. (a) (2, 3) (b) (1, 2) (c) (3, 0) (d) (0, 1) 연속된 두 개의 체인코드가 이와 같은 경우 각각의 체인코드 개수를 1씩 증가시킨다.

Fig. 7. Four conditions of chain code addition for the counter-clockwise border tracing; Each number of expanded border chain codes are added by one if the source border chain codes are (a) (2, 3) or (b) (1, 2) or (c) (3, 0) or (d) (0, 1).

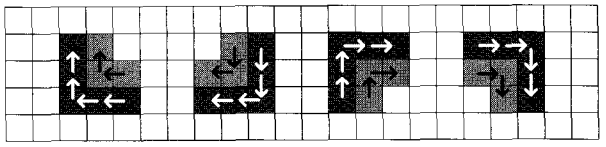

(a) (b) (c) (d)

그림 8. 반 시계 방향의 경계 추적에 있어서 체인코드 감소의 네 가지 경우. (a) (2, 1) (b) (3, 2) (c) (1, 0) (d) (0, 3) 연속된 두 개의 체인코드가 이와 같은 경우 각각의 체인코드 개수를 1씩 감소시킨다.

Fig. 8. Four conditions of chain code reduction for the counter-clockwise border tracing; Each number of expanded border chain codes are reduced by one if the source border chain codes are (a) (2, 1) or (b) (3, 2) or (c) (1, 0) or (d) (0, 3).

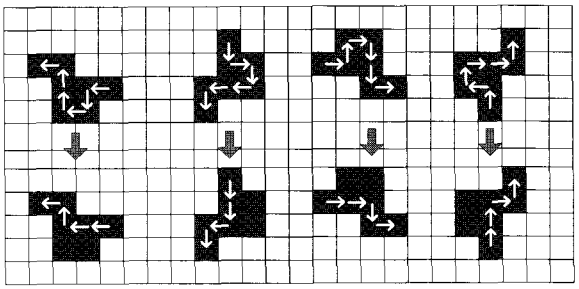

(a) (b) (c) (d)

그림 9. 반 시계 방향의 경계 추적에 있어서 체인코드 제거의 네 가지 경우. (a) (3, 2;1, 1) (b) (0, 3:1, 2) (c) (1, 0:1, 3) (d) (2, 1:1, 0) 연속된 두 개의 체인코드가 이와 같은 경우 각각의 특정 체인 코드를 제거한다.

Fig. 9. Four conditions of chain code removal for the counter-clockwise border tracing; Each number of expanded border chain codes are removed if the source border chain codes are (a) (3, 2:1, 1) or (b) (0, 3:1, 2) or (c) (1, 0:1, 3) or (d) (2, 1:1, 0).

Criterion 3: If connected three chain codes(D_N:nD_N, D_{N+1}:nD_{N+1}, D_{N+2}:nD_{N+2}) are components of a one or two-pixel-wide concave shape(Fig. 9), reduce the number of first and third chain code, nD_N and nD_{N+2}, by min the smaller value between nD_{N+2} and nD_N. Remove chain code if its number is zero. A general description of two connected chain codes which represent a 1-2 pixel wide hollow shape is (D, (D+3)%4:1, (D+2)%4).

3. Starting Position of Expanded Border Tracing

Criterion 4: Move the previous starting position($P1_0$) of border tracing in the direction of the last chain code($D1_F$) addition or reduction and in the opposite direction of the first chain code($D1_0$) addition or reduction. And it is the starting position($P2_0$) of expanded border tracing.

Algorithm 1: Run Length Coding of Inner Border Chain Codes

P_N A Nth inner border pixel element

D_N A chain code value which indicates the direction of the previous move along the border from the previous border element to the current border element

nD_N A number of chain code D_N

1. Pixel P_0 is a starting pixel of the region border that has the minimum column value of all pixel of that region having

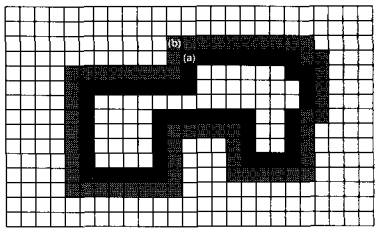

그림 10. 체인코드 기반의 경계 추적에 있어서 추적의 시작점 (a) 실제 경계 (b) 확장된 경계; 경계 확장을 위하여 확장된 경계의 체인코드 기반의 경계 추적을 위한 새로운 시작점을 계산하는 것이 필요하다.

Fig. 10. Starting position of chain code tracing for (a) source border (b) expanded border; A new starting position of chain code tracing of expanded border must be calculated for border expansion.

the minimum row value in the region. Assign D0, the first direction for the neighborhood search, as 3.

2. Search the 3x3 neighborhood of the current pixel in an counter-clockwise direction, beginning the neighborhood search in the pixel position in the direction of $(D_N+3)\ \%\ 4$.
   The first pixel found with the same value as the current pixel is a new boundary element P_N. Update the D_N value.
3. If a border element of one-pixel wide peak shape is found, then add a horizontal direction of top of the peak.

   If $(D_N+D_{N-1})\%4$ is 2,
   add chain code $D=(D_{N-1}+1)\%4$ with $nD=0$.

4. If the current border element P_N is equal to the second border element P_1 and the previous border element P_{N-1} is equal to P_0, then stop. Otherwise repeat setep2 and 3.

Algorithm 2: Border Expansion Algorithm

$P1_0$ A starting pixel of previous border.
$P2_0$ A starting pixel of expanded border
$D1_N$ A Nth run length encoded chain code value of previous border. (N=0~N1)
$nD1_N$ A number of chain code $D1_N$.
$D2_N$ A Nth run length encoded chain code value of expanded borer.
$nD2_N$ A number of chain code $D2_N$.
nC A number of chain codes

1. Search the previous chain code and copy the previous chain code elements($D1_N$:$nD1_N$) to the expanded chain code elements($D2_N$:$nD2_N$) from N=0 to N=nC-1.
   A. If connected two chain codes($D1_{N-1}$, $D1_N$) are components of convex shape, reduce $nD2_{N-1}$, $nD2_N$ by one.
   B. If connected two chain codes($D1_{N-1}$, $D1_N$) are components of concave shape, add $nD2_{N-1}$, $nD2_N$ by one.
   C. If connected three chain codes($D2_{N-2}$, $D2_{N-1}$, $D2_N$) are components of one-pixel-wide concave shape, reduce $nD2_{N-2}$, $nD2_N$ by the smaller value between $nD2_{N-2}$ and $nD2_N$.
2. Searches the expanded chain code for filtering.
   If $nD2_N$ is zero, remove $D2_N$ from the run length coded chain code list and merge two chain codes on both side, $D2_{N-1}$ and $D2_{N+1}$, if they are same.
3. Set the starting pixel $P2_0$ for the expanded border tracing.
   If the first chain code($D2_0$) and the last chain code($D2_{N2}$) of the extended border is same, set $P2_0$ as the directed pixel by the chain code $(D2_0+3)\%4$ from $P1_0$.
   Else, set $P2_0$ as the directed pixel by the chain code $(D2_0+3)\%4$ and $(D2_{N2}+3)\%4$ from $P1_0$.

Algorithm 3: Defect Identification using Border Expansion

1. Search the image from top left until a pixel of a new defect is found; this pixel P_0 then has the minimum column value of all pixels of that region having the minimum row value. If there is not any defect, stop.
2. Get the starting pixel of inner border and the inner border chain codes of a defect using Run length coding of inner border chain codes algorithm(Algorithm 1).
3. Do blob analysis for the founded defect and delete it from the image.
4. Expand border by M time using Border expansion algorithm (Algorithm 2). Where, M is the maximum distance of merging between two distinct blobs in the image.
5. Search the expanded border pixels by the border tracing of run length coded expanded chain codes.
   If an element of new defect is found, set it as new P_0 and opposite direction of last searched expanded chain code as D_0 and repeat step 2, 3 and 4. Merge the feature parameters of child defect to that of the parent defect.
6. Go to step 1.

IV. Experiments

1. System Overview

An AOI system for defect inspection of 5th-generation LCD panel is developed. The optical resolution is 5μm and the target size of defect detection is 8μm.

1.1 Hardware Composition

Fig. 11 is a schematic diagram of the developed AOI system shown in Fig. 12. Line scan type using 12k line CCD cameras is used to cover large size of glass. Lined halogen illumination is used for lighting. Air floating scan bed is developed to reduce any damage during the glass transfer. Precise linear motor and automatic glass aligner are used for glass transferring and aligning. AMD Opteron246 dual-processor and dual-core processing units are used for data processing and PC based interface to control all the hardware components is developed.

1.2 Software Composition

Software part is divided into two groups, Host and Head. Host controls all the system parts and interface with operator. Head is connected to each line scan camera and performs image scanning and image processing for defect defection and classification. Host and Head are connected in network and communicate by sending and receiving messages. Head sends detected defects list to Host after processing is done and Host merges all defects information. The interfaces of the Host and Head software are shown in Fig. 13.

2. Hardware Performance

Hardware performance of the developed AOI system can be evaluated by precision test of image acquisition. Repeatability test is necessary for the estimation of precision. The repeatability test of image acquisition is performed by detecting same defect several times and calculating the standard deviation of detected defect size. Experimental results are shown in Table 3.

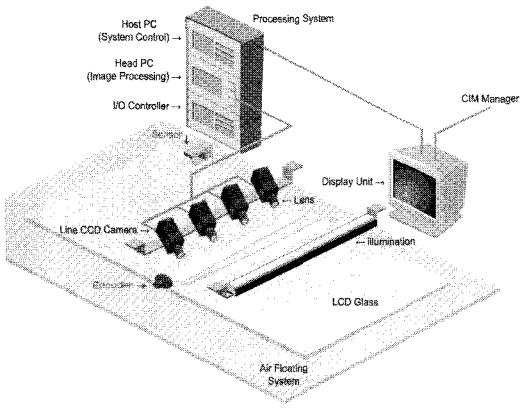

그림 11. 개발된 AOI 시스템의 도식적인 그림.

Fig. 11. A schematic diagram of developed AOI system.

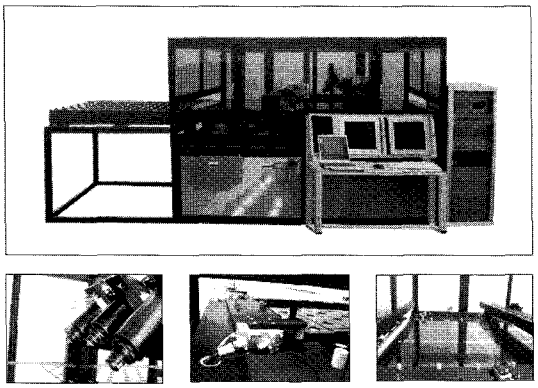

그림 12. 5세대 TFT-LCD 패널의 결함 검사를 위해 개발된 AOI 시스템.

Fig. 12. A developed prototype of AOI system for the defect detection of 5th generation TFT-LCD panels.

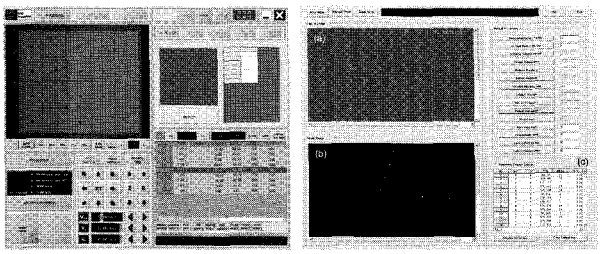

(a) (b)

그림 13. Host와 Head 프로그램 인터페이스 (a) Host 프로그램은 시스템의 모든 부분을 제어하고 작업자와 시스템 사이의 인터페이스를 제공한다. (b) Head 프로그램은 결함 검출을 위한 영상 스캔과 영상 처리를 수행한다.

Fig. 13. Host and Head software interfaces. Host controls all the system parts and interface with operator. Head performs image scanning and image processing for defect defection.

1) Two artificial defects(Fig. 14) are made using laser.
2) The glass is scanned on the developed AOI system by twenty times.
3) Defect detection and identification algorithm is applied to the twenty scanned images.

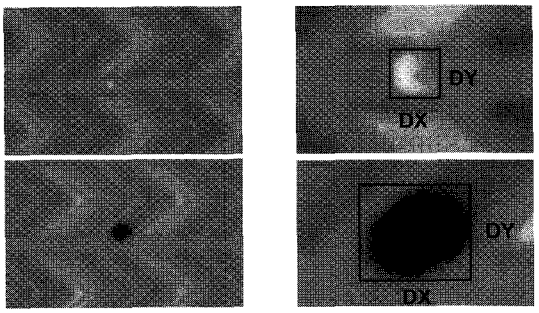

(a) (b)

그림 14. 반복정밀도 측정을 위한 두 개의 샘플 결함. (a) LCD 칼라필터의 결함을 스캔한 영상. (b) 시각화를 위해 (a)를 4배 확대한 영상.

Fig. 14. Two sample defects used for repeatability test. (a) Scanned defective image of LCD color filter panel on the developed AOI system; (b) Four times enlarged image of (a) for visualization.

표 3. 그림14의 샘플 결함의 크기(DX, DY)와 면적에 대한 평균 표준편차. 이 수치는 개발된 AOI 시스템의 반복 정밀도를 나타낸다.

Table 3. Average and standard deviation of defect size(DX, DY) and area of a sample defects shown in Fig. 14. It represents the repeatability of the developed AOI system.

Scan Index	Defect 1 Size		Defect 2 Size		Pattern Period (pixel)
	DX (pixel)	DY (pixel)	DX (pixel)	DY (pixel)	
1	7	6	16	14	59.64
2	6	6	16	14	59.51
3	6	6	16	14	59.65
4	6	7	17	14	59.65
5	6	7	17	14	59.68
6	6	6	17	15	59.46
7	7	6	16	15	59.57
8	7	6	17	14	59.47
9	6	7	16	15	59.40
10	7	6	17	15	59.71
11	7	6	17	14	59.57
12	7	6	17	14	59.53
13	6	6	17	14	59.51
14	7	6	16	14	59.57
15	6	6	16	14	59.54
16	6	6	17	14	59.55
17	6	6	16	14	59.53
18	7	6	16	13	59.53
19	7	6	16	14	59.63
20	6	6	16	14	59.48
AVG	6.45	6.15	16.45	14.15	59.56
STD	0.51	0.37	0.51	0.49	0.08
3σ	1.53	1.10	1.53	1.47	0.24
3σ (μm)	7.65	5.5	7.65	7.35	1.2

4) Defect shape information such as defect position and size are calculated for each image and their standard deviations are calculated (Table 3).
5) The 3-Sigma values(3 · Standard deviation) of defect size represent the repeatability of the developed AOI system(Table 3).

3. Defect Detection Performance

Defect detection performance can be evaluated by the two tests. First, defect detection to check whether the minimum size of detectible defect can be detected or not. Second, comparison of the measured defect size with the real size. The minimum size(8μm) of detectible defect of the developed AOI system is 8μm. Repeated defect detection was performed for the defects in the variable size from 8μm. Each size of detected defects is compared with the real size.

1) The variable size of defects were made using laser. Their size is from 8μm to 34μm in diameter (Fig. 15).
2) The glass is scanned on the developed AOI system several times.
3) Proposed defect identification algorithm (Algorithm 3) is applied on the scanned images.
4) The performance of detecting 8μm defect is confirmed (Fig. 15).
5) The measured defect size is compared with the real size (Table 4).

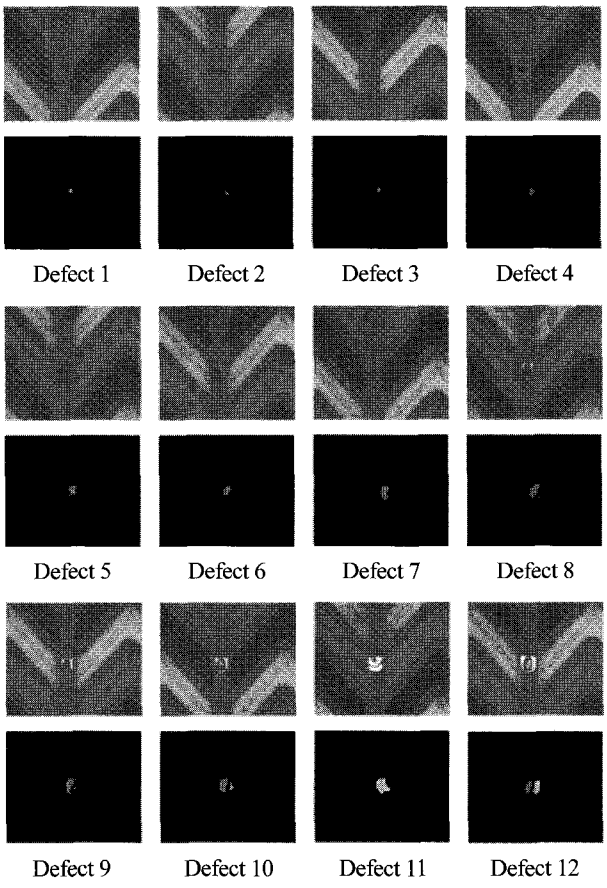

그림 15. 가상의 결함(위쪽 영상)에 대한 개발된 검사 시스템에서의 결함 길출 결과(아래쪽 영상).

Fig. 15. Defect detection results(lower image) of artificial defects (upper image)on the developed inspection system.

표 4. 그림 15의 가상의 결함에 대해 측정된 크기와 실제 크기를 비교하였다.

Table 4. The measured defect size is compared with the real size of the detected defects depicted in Fig. 15.

Index	Real DX, DY (μm)	Real DX, DY (pixel)	Measured DX (pixel)	Measured DY (pixel)
1	8	2	2	2
2	8	2	2	2
3	8	2	2	3
4	12	3	3	3
5	14	3	4	4
6	16	4	4	4
7	18	4	4	6
8	22	5	5	6
9	26	6	5	7
10	28	6	7	7
11	32	7	7	7
12	34	7	8	6
Average of |Real DX - Measured DX|				1.66μm
Average of |Real DY - Measured DY|				3.33μm

4. Processing Time

Processing time of the proposed border expansion algorithm is measured and compared with dilation-erosion algorithm(Fig. 16, Fig. 17). Total processing time of defect detection and identification was measured to evaluate the possibility of in-line application (Fig. 18, Table 5).

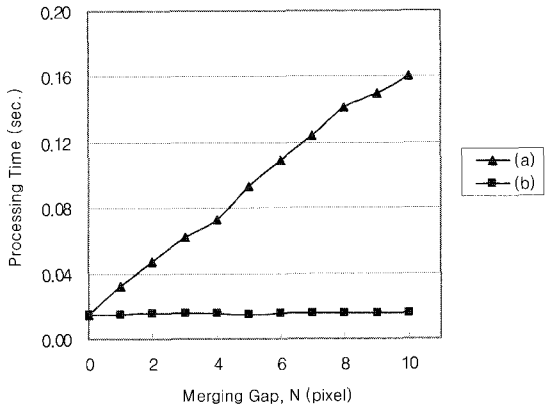

그림 16. 12288×480 크기의 LCD 패널의 패턴영상에서 인접한 결함 영역을 합치는 결합거리에 따른 처리 시간. (a) 침식&팽창 연산을 적용; 결합거리의 증가에 따라 처리 시간이 선형적으로 증가한다. (b) 경계확장 알고리즘을 적용; 처리시간이 결합거리에 무관하게 나타난다.

Fig. 16. Processing time of a 12288×480 patterned LCD panel image versus merging gap. Defect identification is performed using (a) Dilation & Erosion algorithm; processing time increases almost linearly as merging gap increases. (b) Border Expansion algorithm; processing time is almost constant for the merging gap.

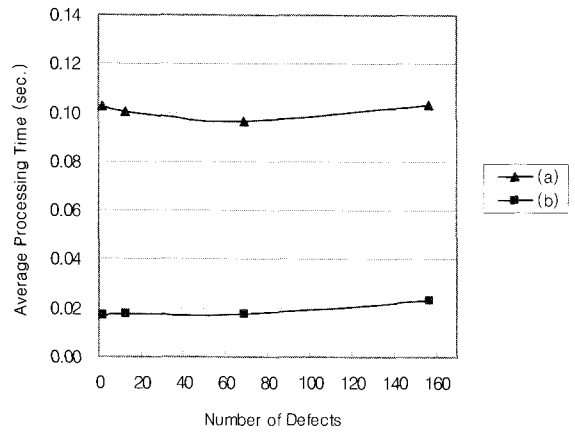

그림 17. 12288×480 크기의 LCD 패널의 패턴영상에 결함 결합거리가 5일 때, 가결함의 개수에 따른 처리 시간. (a) 침식&팽창 연산을 적용. (b) 경계확장 알고리즘을 적용. 이 그래프에서 경계 팽창 알고리즘을 사용하여 결함을 식별하는 경우, 결함의 개수가 60개 이하인 경우에는 처리시간이 거의 동일한 것을 알 수 있다.

Fig. 17. Processing time of a 12288×480 patterned LCD panel image versus the number of defects when the merging gap is 5. Defect identification is performed using (a) Dilation & Erosion, (b) Border Expansion algorithm. This chart demonstrates that the processing time of adjacent defects merging using Border Expansion algorithm is almost independent to the number of defect in the range of 0 to 60.

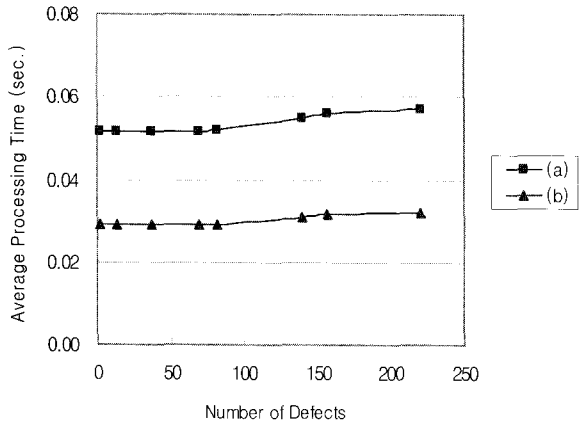

그림 18. 12288×480 크기의 LCD 패널의 패턴영상에 대해 2 방향 근접패턴 비교와 경계확장 알고리즘을 이용하여 결함을 검출하기 위한 처리시간. (a) 단일 스레드로 실행되었을 때; 평균 처리 시간은 0.052초였다. (b) 다중 스레드로 실행되었을 때; 평균 처리 시간은 0.029초였다.

Fig. 18. Processing time of defect detection using two-directional adjacent patterns comparison method and defect identification using border expansion algorithm for a 12288 ×480 patterned LCD panel image. The algorithm is executed in (a) Single thread; Average processing time is 0.052 sec. (b) Multiple thread more than 8; Average processing time is 0.029sec.

표 5. 개발된 AOI 시스템에서 결함을 검사하기 위한 최종 처리시간. 12288 x 480 크기의 LCD 패널의 패턴영상을 처리하는데 0.029초가 소요되었다. 이 시간은 5세대 LCD 패널에 대하여 전체 검사를 1회 스캔에서 16초 안에 가능하게 하고, 2회 스캔에서 32초 안에 가능하게 한다.

Table 5. Total processing time of defect inspection on the developed AOI system. An average processing time of defect inspection for a 12288×480 patterned LCD panel image is 0.029 seconds. It enables total inspection within 16 seconds for one-scan implementation and 32 seconds for two-scan implementation for 5th-generation LCD panel.

Glass Size	5G : 1250 x 1100mm
Resolution	1 pixel = 5μm
Sub-Image Size	61.44 x 2.4mm 2.4 mm in scan direction
Processing Time	0.029sec. for a sub-image
Maximum Scan Speed	2.4mm/0.029sec. = 82.75mm/sec.
Number of Cameras	18 for one-scan implementation 9 for two-scan implementation

V. Conclusion

Currently, a defect inspection system for large size TFT-LCD panel is required to prepare for the coming mass market of digital TV. Machine vision approach is widely used for TFT-LCD inspection and image processing algorithm is the brain of it. In this paper, an overall image processing approach of defect inspection of patterned TFT-LCD panels for the real manufacturing process is presented. The ultimate purpose of the research is to develop an AOI system to inspect the defects in the minimum size of 8μm within 30 seconds for 5th-generation LCD panels.

Hardware performance of developed system is verified by repeatability test. Horizontal repeatability (3σ) of scan image is 6.43μm in the scan direction and 7.65μm normal to the scan direction. Vertical repeatability(3σ) is 1.20μm. Defect detection accuracy was verified by comparing the measured defect size with the real size. Average difference of the measured defect size and the real size is 3.33μm in the scan direction and 1.66μm normal to scan direction. Total processing time for defect detection and identification is 0.029 seconds for 2.4 mm in the scan direction. It enables glass scanning with real-time image processing within 16 seconds for one-step implementation and 32 seconds for two-step implementation for 5th-generation LCD color filter glass. The results show that the developed AOI system which is based on the proposed image processing approach is applicable in the real manufacturing process of TFT-LCD.

References

[1] Burges, J. C. Christopher, A Tutorial on Support Vector Machines for Pattern Recognition. Data Mining and Knowledge Discovery. vol. 2, no. 2, pp. 121-167, 1998.

[2] E. R. Davies, Machine Vision : Theory Algorithms Practicalities. 2nd Edition. (Academic Press), 1997.

[3] Richard O. Duda, Peter E. Hart, and David G. Stork, *Pattern Classification.* New York: Wiley Interscience, 2001.
[4] H. Freeman, "On the encoding of arbitrary geometric configuration." *IRE Transactions on Electronic Computers.* EC-10:260-268, 1961.
[5] G. Renyan, Automatic Defect Inspection and Classification for PDP(Plasma Display Panels). (M.S. Thesis). University of Waterloo, 2003.
[6] E. B. Goldstein, *Sensation & Perception. 4th Edition.* (Sigma Press), 2004.
[7] J. Gil and R. Kimmel, Efficient Dilation, Erosion, Opening and Closing Algorithms. *IEEE Transactions on Pattern Analysis and Machine Intelligence.* vol. 24, no. 12, pp. 1606-1617, 2002.
[8] R. M. Haralick and L. G. Shapiro, *Computer and Robot Vision.* Volume 1. (Addison-Wesley Publishing), 1992.
[9] X. Li and Z. Zhiying, "Group direction difference chain codes for the representation of the border." *Digital and Optical Shape Representation and Pattern Recognition,* SPIE. 938:72-376, 1998.
[10] C.-J. Lu and D.-M. Tsai, Defect inspection of patterned thin film transistor-liquid crystal display panels using a fast sub-image-based singular value decomposition. *International Journal of Production Research.* vol. 42, no. 20, pp. 4333-4351, 2004.
[11] L. Juwei, K. N. Plataniotis (2003) Face Recognition using LDA-based algorithms. *IEEE Transactions on Neural Networks,* vol. 14, pp. 195-200, 2003.
[12] K. Nakashima, "Hybrid Inspection System for LCD Color Filter Panels." *Tenth International Conference of Instrumentation and Measurement Technology.* Hamamatsu, Japen, 1994.
[13] T. M. Mitchell, *Machine Learning.* New York: McGraw-Hill, 1997.
[14] H. Onishi, Y. Sasa, K. Kagai, and S. Tatsumi, "A Parrern Defect Inspection Method by Parallel Grayscale Image Comparison without Precise Image Alignment." *Twenty Eighth Annual Conference of the Industrial Electronics Society,* 2002.
[15] A. Resenfeld and J. Pfaltz, "Sequential Operations in Digital Picture Processing." *Journal of the Association for Computing Machinary.* vol. 13, no. 4, pp. 471-494, 1966.
[16] S. M. Sokolov and A. S. Trekunov, Automatic vision system for final test of liquid crystal display. *International Conference of IEEE Robotics and Automation Society.* Nice, France, 1992.
[17] M. Sonka, V. Hlavac, and R. Boyle, *Image Processing Analysis and Machine Vision.* 2nd Edition. (PWS Publishing), 1999.
[18] W. Tomlinson and B. Halliday, "In-Line SEM based ADC for Advanced Process Control." *2000 IEEE/SEMI Advanced Semiconductor Manufacturing Conference.* pp. 131-137, 2000.
[19] D.-M. Tsai and C.-Y. Hung, "Automatic defect inspection of patterned thin film transistor-liquid crystal display(TFT-LCD) panels using one-dimensional Fourier reconstruction and wavelet decomposition." *International Journal of Production Research.* vol. 43, no. 21, pp. 4589-4607, 2005.
[20] H. Yoda, Y. Ohuchi, Y. Taniguchi, and M. Ejiri, "An Automatic Wafer Inspection System Using Pipelined Image Processing Techniques." IEEE *Transactions on Pattern Analysis and Machine Intelligence.* vol. 10, no. 1, pp. 4-15, 1988.

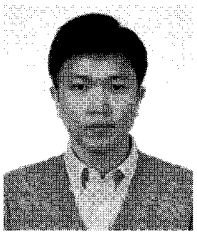

Sung-Bum Kang

received the B.S. degree in Mechanical Engineering with a minor in Electrical Engineering and Computer Science from Kyungpook National University, Korea, in 2004 and M.S. degree in Mechanical Engineering from Seoul National University, Korea, in 2006. He is currently an associate research engineer at SNUPrecision, Co., Ltd. His research interests include machine vision, pattern recognition and micro measurement.

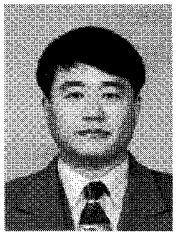

Heui-Jae Pahk

received the B.S. and M.S. degrees in Mechanical Engineering from Seoul National University, Korea, in 1983 and 1985, respectively. Also, he received the Ph.D. degree in Mechanical Engineering from UMIST, UK, in 1990. He is currently a Professor in the School of Mechanical and Aerospace Engineering at Seoul National University. His research interests lie mainly in precision metrology.

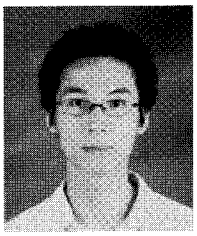

Myung-Sun Lee

received the B.S. degree in Mechanical Engineering from Seoul National University, Korea, in 2005. He is now a Ph.D. candidate in the Mechanical Engineering at Seoul National University. His research interests include machine vision and micro measurement.